Excitation of surface plasmon polariton waves along the direction of periodicity of a one-dimensional photonic crystal

Muhammad Kamran
Department of Electrical Engineering, Lahore University of Management Sciences, Lahore 54792, Pakistan

Muhammad Faryad*
Department of Physics, Lahore University of Management Sciences, Lahore 54792, Pakistan

(Received 8 March 2019; published 8 May 2019)

Excitation of surface plasmon-polariton (SPP) waves was investigated at an interface of a metal and a one-dimensional photonic crystal (1DPC) along the direction of periodicity of the photonic crystal in a prism-coupled configuration. The rigorous coupled-wave approach was used to formulate the problem and the absorptance spectra were obtained as a function of the incidence angle, the period, and the thickness of the photonic crystal. The correlation of the absorptance bands with the underlying canonical problem and the spatial power profiles confirmed the excitation of SPP waves. The excitation of SPP waves at the interface of the 1DPC along the direction of the periodicity opens up new avenues for applications.

DOI: 10.1103/PhysRevA.99.053811

I. INTRODUCTION

The surface plasmon-polariton (SPP) waves are the electromagnetic surface waves guided by an interface of a metal and a dielectric material [1]. The SPP waves are localized to the interface and find applications in sensing and imaging [2]. The idea of electromagnetic surface waves was proposed in 1903 when Uller [3] studied surface waves at the interface of dissipative sea water and air, and in 1907, when Zenneck [4] investigated surface waves guided by an interface of the lossy ground and the lossless air. Surface wave can be excited at an interface between two homogeneous media using a prism-coupled configuration. Turbadar-Otto [5,6] (commonly known as Otto) and Turbadar-Kretschmann-Raether (TKR) [6,7] (commonly known as Kretschmann) configurations are the two types of prism couplings to excite surface waves using evanescent waves that are produced by total internal reflection. A combination of grating and prism couplings can also be used for excitation of SPP waves [8].

Excitation of SPP waves at an interface of a homogeneous material and a one-dimensional photonic crystal (1DPC) was first studied in 1978 [9]. These SPP waves are localized to the interface which is perpendicular to the direction of periodicity of the 1DPC and have several names in the literature like Tamm plasmon-polariton (TPP) waves, surface Bragg waves, or just SPP waves [10]. Surface waves guided by an interface of a metal and a 1DPC have many applications, especially optical sensors of fluids and biochemicals [11,12], light couplers [13], directional emitters [14], and wave guides [15].

In all of this previous work, only the excitation of a surface wave guided by an interface of a homogeneous medium and the photonic crystal was exploited in the direction perpendicular to the periodicity of the 1DPC [15–17]. The excitation of surface waves at the metal-1DPC interface along the direction of periodicity was neglected. Recently, a rigorous formulation of SPP waves' propagation along the direction of the periodicity of the 1DPC was presented in Ref. [18], where they obtained a dispersion equation and solved the canonical boundary-value problem for the excitation of surface waves at the metal-1DPC interface along the direction of periodicity.

However, the canonical boundary-value problem is not practically realizable, because both the partnering materials are supposed to be semi-infinite. And, it is not always possible to assume that the solutions predicted by the canonical problem can be realized in a prism-coupled configuration [19]. Therefore, we set out to investigate if the excitation of the SPP waves at an interface of a metal and a 1DPC along the direction of the periodicity of the photonic crystal in the prism-coupled configuration is possible as predicted by the canonical problem. For this purpose, the prism-coupled problem was formulated using the rigorous coupled-wave approach (RCWA) [20,21].

The plan of this paper is as follows: The description and brief formulation of the problem are given in Sec. II. Numerical results are presented and discussed in Sec. III and concluding remarks are presented in Sec. IV. An $\exp(-i\omega t)$ time dependence is implicit in the paper, where ω is the angular frequency and t is the time. The free-space wavelength and free-space wave number are denoted by $\lambda_0 = 2\pi/k_0$ and $k_0 = \omega\sqrt{\varepsilon_0\mu_0}$, respectively, where ε_0 and μ_0 are the permittivity and permeability of free space. Vectors are in bold and unit vectors are additionally denoted by a hat. The Cartesian unit vectors are denoted by $\hat{\mathbf{u}}_\mathbf{x}$, $\hat{\mathbf{u}}_\mathbf{y}$, and $\hat{\mathbf{u}}_\mathbf{z}$. The column vectors are in bold and inside square brackets, whereas matrices are double underlined and enclosed in square brackets. The asterisk represents a complex conjugate.

*Corresponding author: muhammad.faryad@lums.edu.pk

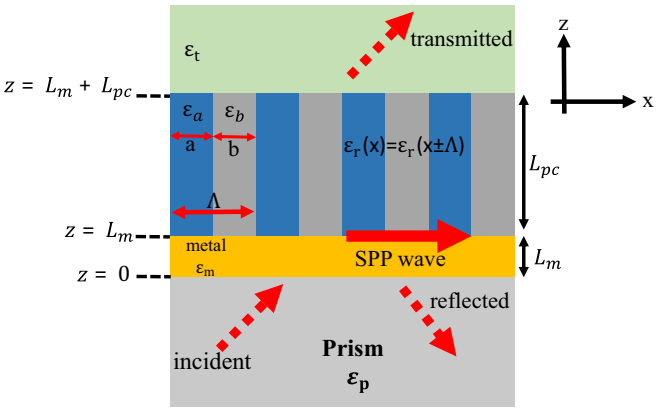

FIG. 1. Schematic representation of the geometry of the boundary-value problem. A p-polarized plane wave is incident upon the metal-1DPC bilayer from inside a prism of relative permittivity ε_p.

II. PROBLEM DESCRIPTION

Let us consider the geometry of the problem schematically shown in Fig. 1. Let us assume that the SPP wave is guided by the interface of the metal and the 1DPC along the x axis. Let the half space $z < 0$ be occupied by homogeneous medium (prism) with permittivity ε_p. The region $0 < z < L_m$ is occupied by a metal with permittivity ε_m and thickness L_m. The region between $z > L_m$ and $z < L_m + L_{pc}$ is a photonic crystal of period Λ and thickness L_{pc}. The relative permittivity of the photonic crystal is

$$\varepsilon_r(x) = \varepsilon_r(x \pm \Lambda)\,, \quad L_m < z < L_m + L_{pc}\,. \tag{1}$$

The permittivity of the photonic crystal can be expanded as a Fourier series with respect to x,

$$\varepsilon_r(x) = \sum_{\ell\in\mathbb{Z}} \varepsilon_r^{(\ell)} \exp(i\ell\kappa_x x)\,, \quad \mathbb{Z} \in \{0, \pm1, \pm2, \ldots\}\,, \tag{2}$$

where $\kappa_x = 2\pi/\Lambda$, and

$$\varepsilon_r^{(0)} = \frac{1}{\Lambda}\int_0^\Lambda \varepsilon_r(x)dx\,, \tag{3}$$

and

$$\varepsilon_r^{(\ell)} = \frac{1}{\Lambda}\int_0^\Lambda \varepsilon_r(x)\exp(-i\ell\kappa_x x)dx\,, \quad \ell \neq 0\,. \tag{4}$$

The region $z > L_m + L_{pc}$ is a semi-infinite medium with permittivity ε_t.

To predict the excitation of the SPP waves we need to compute the plane-wave absorption by the metal and the 1DPC and identify the absorption peaks that are independent of the thickness of the photonic crystal. Since the 1DPC is taken to be made up of isotropic materials, only a p-polarized incident plane wave can excite an SPP wave. For this purpose, let us consider a p-polarized plane wave propagating in the xz plane and that is incident on the metal from the prism side, making an angle θ with the z axis. The incident, reflected, and transmitted electric field phasors are given by

$$\mathbf{E}_{\rm inc}(\mathbf{r}) = \hat{\mathbf{p}}_0^+ a_p^{(0)} \exp\left\{i\left[k_x^{(0)}x + k_{zp}^{(0)}z\right]\right\}, \quad z < 0\,, \tag{5}$$

$$\mathbf{E}_{\rm ref}(\mathbf{r}) = \sum_{\ell=-N_t}^{N_t} \hat{\mathbf{p}}_\ell^- r_p^{(\ell)} \exp\left[i\left(k_x^{(\ell)}x - k_{zp}^{(\ell)}z\right)\right], \quad z < 0\,, \tag{6}$$

and

$$\mathbf{E}_{\rm tr}(\mathbf{r}) = \sum_{\ell=-N_t}^{N_t} \hat{\mathbf{p}}_\ell^t t_p^{(\ell)} \exp\left(i\left\{k_x^{(\ell)}x + k_{zt}^{(\ell)}[z - (L_m + L_{pc})]\right\}\right), \quad z > L_m + L_{pc}, \tag{7}$$

respectively, in terms of the Floquet harmonics, where $a_p^{(0)}$ is the known amplitude of the incident electric field, and $r_p^{(\ell)}$ and $t_p^{(\ell)}$ are the unknown field amplitude of the reflected and transmitted electric fields of the ℓth Floquet harmonics, where ℓ is the order of the Floquet harmonics with $\ell \in \{0, \pm1, \pm2, \ldots\}$. Here $\ell = 0$ represents the specular component of the fields, and $\ell \neq 0$ are the nonspecular components of the fields. Other parameters are given by

$$k_{zp}^{(\ell)} = \sqrt{k_0^2\varepsilon_p - \left(k_x^{(\ell)}\right)^2}\,, \tag{8}$$

$$k_{zt}^{(\ell)} = \sqrt{k_0^2\varepsilon_t - \left(k_x^{(\ell)}\right)^2}\,, \tag{9}$$

$$\hat{\mathbf{p}}_\ell^\pm = \frac{\mp k_{zp}^{(\ell)}\hat{\mathbf{u}}_x + k_x^{(\ell)}\hat{\mathbf{u}}_z}{k_0\sqrt{\varepsilon}_p}\,, \tag{10}$$

and

$$\hat{\mathbf{p}}_\ell^t = \frac{k_{zt}^{(\ell)}\hat{\mathbf{u}}_x + k_x^{(\ell)}\hat{\mathbf{u}}_z}{k_0\sqrt{\varepsilon}_t}\,. \tag{11}$$

The x component of the wave number is given by

$$k_x^{(\ell)} = k_0\sqrt{\varepsilon}_p \sin\theta + \ell(2\pi/\Lambda)\,. \tag{12}$$

To implement the RCWA, the field phasors are expanded in terms of Floquet harmonics in the region $0 \leqslant z \leqslant L_m + L_{pc}$ as

$$\mathbf{E}(\mathbf{r}) = \sum_{\ell=-N_t}^{N_t} \left[E_x^{(\ell)}(z)\hat{\mathbf{u}}_x + E_z^{(\ell)}(z)\hat{\mathbf{u}}_z\right] \times \exp\left(ik_x^{(\ell)}x\right), \quad z \in [0, L_m + L_{pc}]\,, \tag{13}$$

$$\mathbf{H}(\mathbf{r}) = \sum_{\ell=-N_t}^{N_t} H_y^{(\ell)}(z)\hat{\mathbf{u}}_y \exp\left(ik_x^{(\ell)}x\right)\Big], \quad z \in [0, L_m + L_{pc}]\,, \tag{14}$$

where N_t is an integer. Substituting Eqs. (13) and (14) in Maxwell curl postulates, we get two ordinary differential equations and one algebraic equation. The algebraic equation can be arranged as

$$\left[\mathbf{E_z}(\mathbf{z})\right] = -\frac{\eta_0}{k_0}\left[\underline{\underline{\varepsilon}}(z)\right]^{-1} \cdot \left[\underline{\underline{K}}_x\right] \cdot \left[\mathbf{H_y}(\mathbf{z})\right], \tag{15}$$

where

$$\left[\underline{\underline{K}}_x\right] = \mathrm{diag}\left[k_x^{(\ell)}\right] \tag{16}$$

is a $(2N_t + 1) \times (2N_t + 1)$ diagonal matrix,

$$\left[\underline{\underline{\varepsilon}}(z)\right] = \left[\varepsilon^{(\ell-m)}(z)\right] \tag{17}$$

is a $(2N_t+1)\times(2N_t+1)$ Toeplitz matrix, and $[\mathbf{E}_x(z)]$, etc., are $(2N_t+1)\times 1$ column matrices. The two differential equations can be rearranged as a matrix ordinary differential equation

$$\frac{d}{dz}[\mathbf{f}^{(p)}(z)] = i[\underline{\underline{P}}^{(p)}(z)]\cdot[\mathbf{f}^{(p)}(z)]\,, \qquad z\in(0, L_m+L_{pc})\,, \tag{18}$$

where the $2(2N_t+1)\times 1$ column vector $[\mathbf{f}^{(p)}(z)]$ is given as

$$[\mathbf{f}^{(p)}(z)] = [\mathbf{E}_x(z)]^T, \eta_0[\mathbf{H}_y(z)]^{T\,T}\,, \tag{19}$$

and

$$[\underline{\underline{P}}^{(p)}(z)] = \begin{bmatrix} [\underline{0}] & [\underline{\underline{P}}_{14}(z)] \\ [\underline{\underline{P}}_{41}(z)] & [\underline{0}] \end{bmatrix}, \tag{20}$$

where $[\underline{0}]$ and $[\underline{I}]$ are the $(2N_t+1)\times(2N_t+1)$ null and identity matrices, respectively, and

$$[\underline{\underline{P}}_{14}(z)] = k_0[\underline{I}] - \frac{1}{k_0}[\underline{\underline{K}}_x]\cdot[\underline{\underline{\varepsilon}}(z)]^{-1}\cdot[\underline{\underline{K}}_x]\,, \tag{21}$$

$$[\underline{\underline{P}}_{41}(z)] = k_0[\underline{\underline{\varepsilon}}(z)]\,. \tag{22}$$

The matrix $[\underline{\underline{P}}^{(p)}(z)]$ in Eq. (18) is z dependent. In order to solve this differential equation, the region between $0\leqslant z\leqslant L_m+L_{pc}$ is divided into small parallel slices, so that in each slice the matrix $[\underline{\underline{P}}^{(p)}(z)]$ remains constant. The region $0\leqslant z\leqslant L_m$ is divided into N_m slices, and the region $L_m\leqslant z\leqslant L_m+L_{pc}$ is divided into N_{pc} slices. A stable algorithm provided in Refs. [22–24] is then used to compute the reflection and transmission amplitudes. The continuity of the fields in $[\mathbf{f}^{(p)}(z)]$ is implemented at the interfaces at $z=0$, $z=L_m$, and $z=L_m+L_{pc}$.

Linear reflectance and transmittance are defined as

$$R_{pp}^{(\ell)} = \left|\frac{r_p^{(\ell)}}{a_p^{(0)}}\right|^2 \frac{\mathrm{Re}\big[k_{zp}^{(\ell)}\big]}{k_{zp}^{(0)}}\,, \tag{23}$$

and

$$T_{pp}^{(\ell)} = \left|\frac{t_p^{(\ell)}}{a_p^{(0)}}\right|^2 \frac{\mathrm{Re}\big[k_{zt}^{(\ell)}\big]}{k_{zp}^{(0)}}\,, \tag{24}$$

respectively, so that the absorptance is

$$A_p = 1 - \sum_{\ell=-N_t}^{N_t}\left(R_{pp}^{(\ell)} + T_{pp}^{(\ell)}\right). \tag{25}$$

The reflection and transmission amplitudes are found using the RCWA using a stable algorithm [22,23,25,26].

III. NUMERICAL RESULTS AND DISCUSSION

For representative numerical results, the 1DPC is taken to be the same as in Ref. [18] for comparison of the results in this paper with those of the underlying canonical problem solved in Ref. [18]. The 1DPC is made up of alternating layers of two dielectric media with thicknesses a and b, and relative permittivities ε_a and ε_b, respectively. Both the layers are of equal thicknesses so that $a=b=0.5\Lambda$ and the relative permittivity is

$$\varepsilon_r(x) = \begin{cases} \varepsilon_a\,, & 0<x<0.5\Lambda \\ \varepsilon_b\,, & 0.5\Lambda<x<\Lambda. \end{cases} \tag{26}$$

The Fourier coefficients for this permittivity profile are given as

$$\begin{aligned} \varepsilon_r^{(0)} &= \frac{\varepsilon_a+\varepsilon_b}{2}\,, \\ \varepsilon_r^{(\ell)} &= \frac{i(\varepsilon_b-\varepsilon_a)}{\ell\pi}\,, \quad \forall\ \ell=\text{odd}\,, \\ \varepsilon_r^{(\ell)} &= 0\,, \quad \forall\ \ell=\text{even}\,. \end{aligned} \tag{27}$$

For the numerical results in this section, the free-space wavelength is fixed at $\lambda_0=633$ nm. The metal is chosen to be gold with the relative permittivity $\varepsilon_m=-11.8+1.3i$ and thickness $L_m=10$ nm. The parameter N_t in the summations is set to be 15 after ascertaining the convergence of the results within 0.5% of the results when $N_t=14$. Also, $N_m=1$ and $N_{pc}=1$ were set for the computation of the absorptance

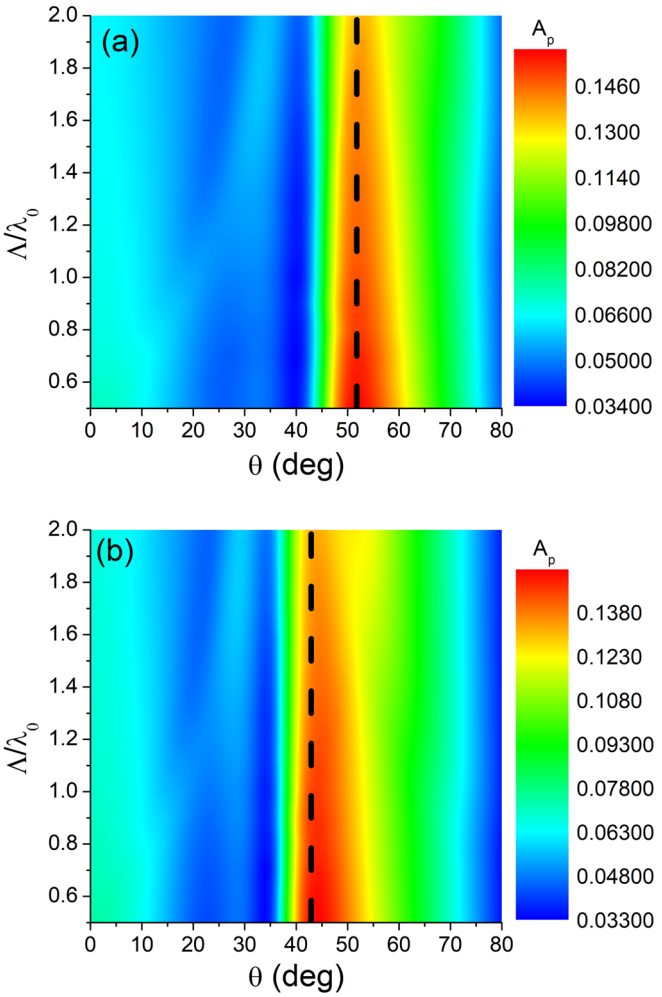

FIG. 2. Absorptance A_p as a function of incidence angle θ and the period Λ of the 1DPC, when $L_m=10$ nm, $L_{pc}=250$ nm, $n_t=n_p$, and (a) $n_p=2.6$ and (b) $n_p=3.0$. The black dashed line represents the angle of incidence for the excitation of surface waves in the underlying canonical boundary-value problem predicted using Eq. (28).

since both the metal and the 1DPC are homogeneous along the z axis. The relative permittivities of the alternating layer in the 1DPC are taken to be $\varepsilon_a = (n_a)^2 + 10^{-6}i$ and $\varepsilon_b = (n_b)^2 + 10^{-6}i$, where $n_a = 1.5$ and $n_b = 2$. The reason behind choosing these values of n_a and n_b is that most of the dielectric materials have their refractive indices around it in the visible range. For instance, many silica-based glasses have their refractive index as 1.5 and the refractive index of ZnO is 2 at a wavelength of 633 nm. The small imaginary part 10^{-6} is added for comparison with the canonical problem where it was required for the computational purpose. The small imaginary part also models the real materials more accurately as all materials are lossy even though the losses are small in dielectric materials. The refractive index of the transmission medium $n_t = \sqrt{\varepsilon_t}$ is taken to be the same as that of the prism.

To delineate the excitation of SPP waves, the absorptance spectrum A_p as a function of the incidence angle θ and the period Λ of the 1DPC is presented in Fig. 2(a) for a prism with refractive index $n_p = 2.6$ and thickness of the 1DPC $L_{pc} = 250$ nm. A quick scan of the figure shows that an absorptance band around $\theta = 52^\circ$ is present which indicates the excitation of an SPP wave. To confirm that this absorptance band correlates with the canonical problem, we can use Eq. (12) to find the θ predicted by the canonical problem as

$$\theta = \sin^{-1}\left[\frac{\mathrm{Re}(q) - \ell(2\pi/\Lambda)}{k_0 n_p}\right], \tag{28}$$

where $q \sim 2.04k_0$ is the wave number predicted by the canonical problem [18]. For the parameters used in Fig. 2(a), Eq. (28) gives $\theta \sim 51.8^\circ$ when $\ell = 0$, which is in excellent agreement with the position of the spectral band found at $\theta = 52^\circ$. Therefore, it can be concluded that the SPP wave is being excited as a Floquet harmonic of order zero.

To see the effect of the refractive index of the prism, the absorptance was computed for a prism with $n_p = 3.0$ [all other parameters are the same as in Fig. 2(a)] and is presented in Fig. 2(b). Now, the absorptance band shifts to $\theta \sim 44^\circ$. The canonical problem predicts the excitation angle of $\theta \sim 42.9^\circ$

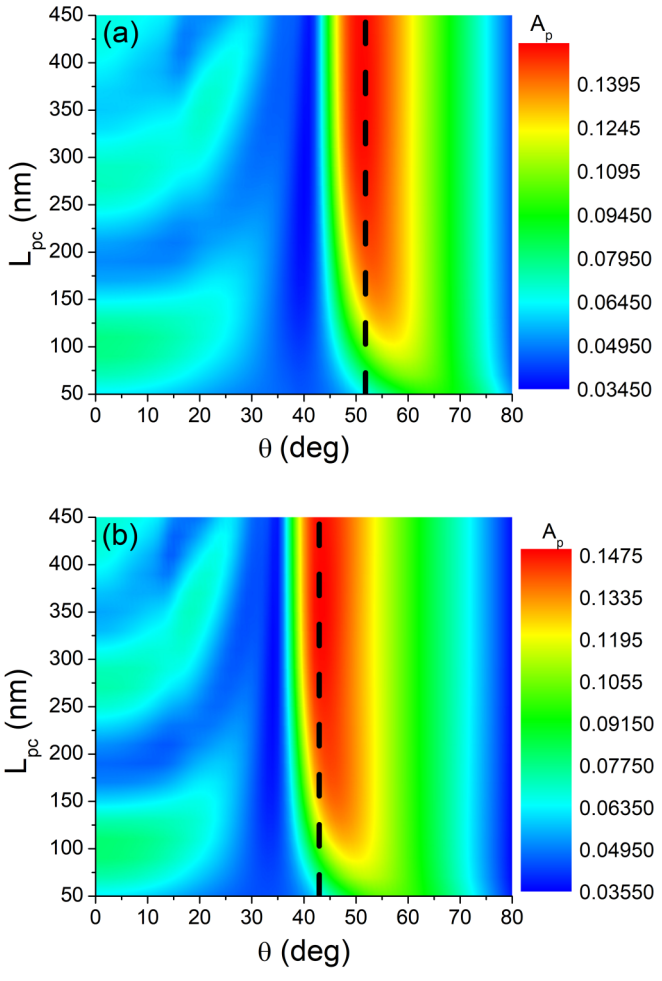

FIG. 3. Absorptance A_p as a function of incidence angle θ and the thickness L_{pc} of the 1DPC when $L_m = 10$ nm, $\Lambda = 1.0\lambda_0$ nm, $n_t = n_p$, and (a) $n_p = 2.6$ and (b) $n_p = 3.0$. The black dashed line represents the angle of incidence for the excitation of surface waves in the underlying canonical boundary-value problem predicted using Eq. (28).

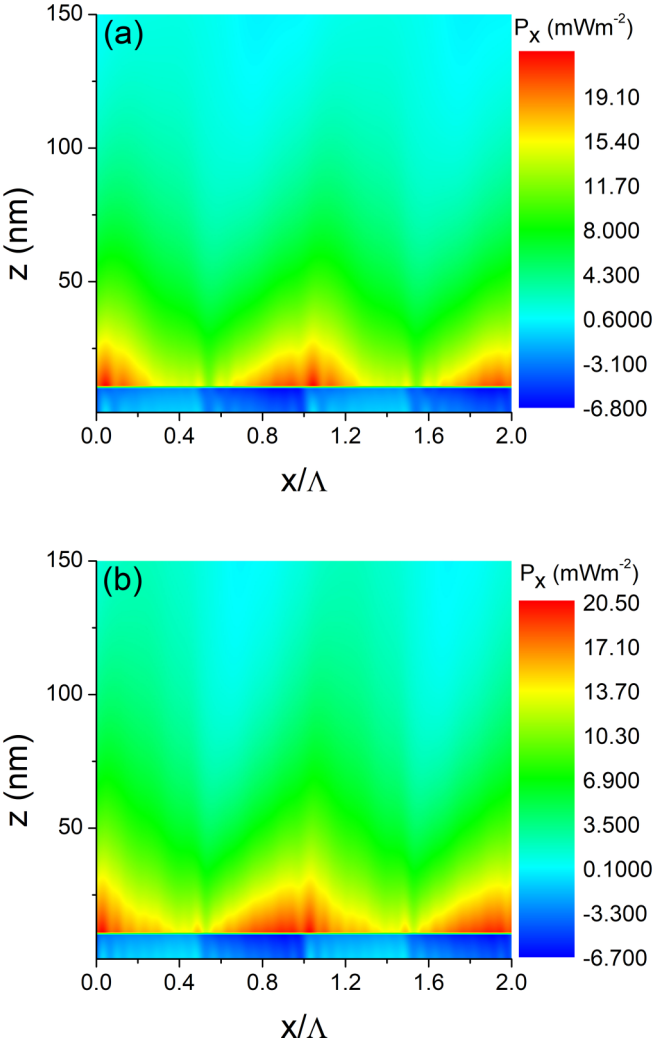

FIG. 4. Variation of the x component of the time-averaged Poynting vector P_x as a function of x and z, when $L_m = 10$ nm, $L_{pc} = 250$ nm, $n_p = 3.0$, $n_t = n_p$, $\theta = 44^\circ$, and (a) $\Lambda = 1.0\lambda_0$ and (b) $\Lambda = 1.5\lambda_0$.

that is still in excellent agreement with the angular location of our absorptance band.

To understand the effect of the thickness of the photonic crystal, the absorptance is presented in Fig. 3 as a function of the incidence angle θ and the thickness L_{pc} of the 1DPC for two values of the refractive index of the prism when $\Lambda = 1.0\lambda_0$. The slight change in the incidence angle when the thickness of the photonic crystal increases is because of the fact that the SPP wave is localized to the interface on the photonic crystal side and is extended to about 100 nm as the location of the absorption band stops changing after the thickness is increased beyond 100 nm.

To check the spatial extent of the SPP waves on both sides of the interface, the time-averaged Poynting vector is computed at the incidence angle where the surface wave is excited. For this purpose, the electric and magnetic field phasors are computed by dividing the photonic crystal and the metallic layer into 1-nm-thick slices parallel to the metal-1DPC interface. Therefore, for the field and Poynting vector computation, the values of $N_m = L_m/1$ nm and $N_{pc} = L_{pc}/1$ nm were taken so as to get 1-nm resolution on the z axis. Furthermore, $a_p = 1\ \mathrm{V\,m^{-1}}$ was set. Across each slice, the field vector is computed by the solution of Eq. (18) as

$$[\mathbf{f}^{(p)}(z_j)] = \exp[i[\underline{\underline{P}}^{(p)}](z_j - z_{j-1})]\cdot[\mathbf{f}^{(p)}(z_{j-1})]\,, \quad j \in \{1, N_m + N_{pc}\}. \tag{29}$$

After using the components of the field phasors in Eqs. (13) and (14), the x component of the time-averaged Poynting vector is given by

$$\mathbf{P}_x(x,z) = \tfrac{1}{2}\mathrm{Re}[\mathbf{E}(x,z) \times \mathbf{H}^*(x,z)] \tag{30}$$

and is presented in Figs. 4(a) and 4(b) when $\Lambda = 1.0\lambda_0$ and $1.5\lambda_0$, respectively, and $\theta = 44^\circ$, $L_{pc} = 250$ nm, and $n_p = 3.0$. We can observe that the power density is localized to the metal-1DPC interface which is an indication of the excitation of surface waves. Furthermore, on the side of the photonic crystal, the power is localized to about 100 nm from the interface. This is in line with the conclusion drawn from Fig. 3.

IV. CONCLUDING REMARKS

The excitation of SPP waves guided by the interface of a metal and a 1DPC was shown along the interface which contains the direction of periodicity of the photonic crystal. A prism-coupled configuration was used to excite the SPP waves using metallic films and the 1DPC of the finite width. Those absorptance bands were identified for plane-wave incidence that remains unchanged by a change in the thickness of the 1DPC. The absorptance bands computed using the RCWA agreed excellently with the prediction of the canonical boundary-value problem. The spatial profiles of the power density showed an excellent localization of the SPP waves to the metal-1DPC interface. The excitation angle in the prism-coupled configuration is in full agreement with the dispersion relation developed for this problem in our earlier work [18].

In contrast to the SPP waves guided by an interface of a metal and a 1DPC which is perpendicular to the direction of periodicity of the photonic crystal, this work established the excitation of the SPP waves on the long-neglected interface along the direction of the periodicity. It is hoped that it will open up new avenues of the applications in sensing and imaging. Let us also note that multiple SPP waves of different wave numbers were excited when the direction of periodicity of the photonic crystal was perpendicular to the interface [25,27,28] but no such multiplicity exists in the present case.

ACKNOWLEDGMENT

Higher Education Commission, Pakistan, partially supported this work via Grant No. NRPU 2016-5905.

[1] H. Raether, *Surface Plasmons on Smooth and Rough Surfaces and on Gratings* (Springer-Verlag, Berlin, 1988).
[2] S. A. Maier, *Plasmonics: Fundamentals and Applications* (Springer, Berlin, 2007).
[3] K. Uller, Ph.D. thesis, Universita Rostock, 1903.
[4] J. Zenneck, Ann. Phys. (Leipzig) **23**, 846 (1907).
[5] A. Otto, Z. Phys. **216**, 398 (1968).
[6] T. Turbadar, Proc. Phys. Soc. **73**, 40 (1959).
[7] E. Kretschmann and H. Raether, Z. Naturforsch. A **23**, 2135 (1968).
[8] M. Kamran and M. Faryad, Plasmonics (2018), doi: 10.1007/s11468-018-0859-3.
[9] P. Yeh, A. Yariv, and A. Y. Cho, App. Phys. Lett. **32**, 104 (1978).
[10] M. Kaliteevski, I. Iorsh, S. Brand, R. A. Abram, J. M. Chamberlain, A. V. Kavokin, and I. A. Shelykh, Phys. Rev. B **76**, 165415 (2007).
[11] V. N. Konopsky and E. V. Alieva, Anal. Chem. **79**, 4729 (2007).
[12] M. Skorobogatiy and A. V. Kabashin, Appl. Phys. Lett. **89**, 143518 (2006).
[13] E. Morino, L. Martín-Morino, and F. J. García-Vedal, Photonics Nanostruct. **2**, 97 (2004).
[14] P. Kramper, M. Agio, C. M. Soukoulis, A. Birner, F. Muller, R. B. Wehrspohn, U. Gosele, and V. Sandoghdar, Phys. Rev. Lett. **92**, 113903 (2004).
[15] H. K. Baghbadorani, D. Aurelio, J. Barvestani, and M. Liscidini, J. Opt. Soc. Am. B **35**, 805 (2018).
[16] R. D. Meade, K. D. Brommer, A. M. Rappe, and J. D. Joannopoulos, Phys. Rev. B **44**, 10961 (1991).
[17] J. Barvestani, M. Kalafi, A. Soltani-Vala, and A. Namdar, Phys. Rev. A **77**, 013805 (2008).
[18] M. Rasheed and M. Faryad, J. Opt. Soc. Am. B **35**, 2957 (2018); **36**, 1396 (2019).

[19] M. Faryad and A. Lakhtakia, J. Opt. Soc. Am. B **31**, 1706 (2014).
[20] E. N. Glytsis and T. K. Gaylord, J. Opt. Soc. Am. A **4**, 2061 (1987).
[21] N. Chateau and J. P. Hugonin, J. Opt. Soc. Am. A **11**, 1321 (1994).
[22] M. Faryad and A. Lakhtakia, Phys. Rev. A **84**, 033852 (2011).
[23] M. G. Moharam, E. B. Grann, D. A. Pommet, and T. K. Gaylord, J. Opt. Soc. Am. A **12**, 1068 (1995).
[24] F. Wnag, M. W. Horn, and A. Lakhtakia, Microelectron. Eng. **71**, 34 (2004).
[25] J. A. Polo, Jr., T. G. Mackay, and A. Lakhtakia, *Electromagnetic Surface Waves: A Modern Perspective* (Elsevier, Amsterdam, 2013).
[26] L. Li, J. Opt. Soc. Am. A **10**, 2581 (1993).
[27] M. Faryad and A. Lakhtakia, J. Opt. Soc. Am. B **27**, 2218 (2010).
[28] M. Faryad, Appl. Phys. A **124**, 102 (2018).